Diabetologia (2013) 56:2638–2646
DOI 10.1007/s00125-013-3044-4

ARTICLE

Pathological endoplasmic reticulum stress mediated by the IRE1 pathway contributes to pre-insulitic beta cell apoptosis in a virus-induced rat model of type 1 diabetes

Chaoxing Yang · Philip diIorio · Agata Jurczyk · Bryan O'Sullivan-Murphy · Fumihiko Urano · Rita Bortell

Received: 14 June 2013 / Accepted: 15 August 2013 / Published online: 13 September 2013

Abstract
Aims/hypothesis We hypothesised that pathological endoplasmic reticulum (ER) stress contributes to beta cell death during development of type 1 diabetes. In this study, we investigated the occurrence of beta cell ER stress and the signalling pathways involved during discrete stages of autoimmune diabetes progression. The virus-inducible BBDR rat model was used to systematically interrogate the three main ER stress signalling pathways (IRE1 [inositol-requiring protein-1], PERK [double-stranded RNA-dependent protein kinase (PKR)-like ER kinase] and ATF6 [activating transcription factor 6]) in pancreatic beta cells during type 1 diabetes development.

Methods ER stress and apoptotic markers were assessed by immunoblot analyses of isolated pancreatic islets and immunofluorescence staining of pancreas sections from control and virus-induced rats. Various time points were analysed: (1) early stages preceding the development of insulitis and (2) a late stage during onset and progression of insulitis, which precedes overt hyperglycaemia.
Results The IRE1 pathway, including its downstream component X-box-binding protein 1, was specifically activated in pancreatic beta cells of virus-induced rats at early stages preceding the development of insulitis. Furthermore, ER stress-specific pro-apoptotic caspase 12 and effector caspase 3 were also activated at this stage. Activation of PERK and its downstream effector pro-apoptotic CHOP (CCAAT/-enhancer-binding-protein homologous protein), only occurred during late stages of diabetes induction concurrent with insulitis, whereas ATF6 activation in pancreatic beta cells was similar in control and virus-induced rats.
Conclusions/interpretation Activation of the IRE1 pathway and ER stress-specific pro-apoptotic caspase 12, before the development of insulitis, are indicative of ER stress-mediated beta cell damage. The early occurrence of pathological ER stress and death in pancreatic beta cells may contribute to the initiation and/or progression of virus-induced autoimmune diabetes.

Keywords Apoptosis · BB rat · Beta cell · ER stress · IRE1 pathway · Type 1 diabetes · Virus

Abbreviations

ATF6	Activating transcription factor 6
BBDR	BioBreeding Diabetes Resistant
CHOP	CCAAT/-enhancer-binding-protein homologous protein
ER	Endoplasmic reticulum

Electronic supplementary material The online version of this article (doi:10.1007/s00125-013-3044-4) contains peer-reviewed but unedited supplementary material, which is available to authorised users.

C. Yang · P. diIorio · A. Jurczyk · R. Bortell (✉)
Program in Molecular Medicine, University of Massachusetts Medical School, 368 Plantation Street, AS7-2055, Worcester, MA 01605, USA
e-mail: rita.bortell@umassmed.edu

C. Yang · P. diIorio · A. Jurczyk · R. Bortell
Diabetes Center of Excellence, University of Massachusetts Medical School, Worcester, MA, USA

B. O'Sullivan-Murphy
Program in Gene Function and Expression, University of Massachusetts Medical School, Worcester, MA, USA

F. Urano
Division of Endocrinology, Metabolism, and Lipid Research, Washington University School of Medicine, St Louis, MO, USA

F. Urano
Department of Medicine, Washington University School of Medicine, St Louis, MO, USA

H&E	Haematoxylin and eosin
IRE1	Inositol-requiring protein-1
KRV	Kilham rat virus
PERK	PKR-like ER kinase
pIC	Polyinosinic:polycytidylic acid
PKR	Double-stranded RNA-dependent protein kinase
TBST	Tris-buffered saline Tween
UPR	Unfolded protein response
XBP-1	X-box-binding protein 1

Introduction

Pancreatic beta cells have a highly developed endoplasmic reticulum (ER) in order to meet the heavy demand for insulin biosynthesis. Rapid changes in insulin requirements and/or deleterious alterations in the beta cells' environment may cause accumulation of misfolded proteins and lead to a cellular adaptive response termed the unfolded protein response (UPR) [1]. Three ER transmembrane proteins are known to sense ER stress: IRE1 (inositol-requiring protein-1), PERK (double-stranded RNA-dependent protein kinase [PKR]-like ER kinase) and ATF6 (activating transcription factor 6). Each of these transducers activates separate, but integrated, arms of the UPR to mitigate ER stress by decreasing protein translation, degrading misfolded proteins and increasing the levels of ER-resident chaperones to aid in protein folding [2–4]. Under conditions of unresolved ER stress, however, the UPR may initiate an ER stress-mediated apoptotic pathway [5]. Thus, the UPR may serve to underlie both physiological and pathological functions.

Unresolvable ER stress has been proposed to play a role in beta cell death during the progression of both type 1 and type 2 diabetes based on in vitro studies [6–9]. In support of this, pancreatic islets of patients with type 2 diabetes are more susceptible to high-glucose-induced ER stress than islets from non-diabetic controls [9] and, recently, increased levels of a few ER stress markers were found in islets from individuals with type 1 diabetes compared with non-diabetic controls [10]. A report in the NOD mouse, a well-studied animal model of spontaneous autoimmune diabetes, demonstrates that beta cell ER stress occurs in 6- to 10-week-old female mice before the onset of diabetes [11]. However, because of the incomplete penetrance (~70%) and variable time to insulitis and onset of hyperglycaemia in this model, it is difficult to conclude whether beta cell ER stress contributes to, or is merely a consequence of, autoimmunity development. To elucidate this, we used the virus-inducible BioBreeding Diabetes Resistant (BBDR) rat, which develops autoimmune diabetes at levels approaching 100% in ~2 weeks following infection [12, 13]. Because the appearance of insulitis and subsequent development of hyperglycaemia follow predictable kinetics, this rat model allowed us to investigate ER stress signalling in pancreatic beta cells at discrete time points both before and during insulitis (lymphocytic infiltration of islets), the hallmark of autoimmunity.

Methods

Animals BBDR rats were bred at the University of Massachusetts or obtained from BRM (Worcester, MA, USA). Rats were housed in a viral-antibody-free facility and maintained in accordance with the Guide for the Care and Use of Laboratory Animals (Institute of Laboratory Animal Resources, 1996) and guidelines of our Institutional Animal Care and Use Committee.

Diabetes induction BBDR rats of either sex and 21–24 days old were injected intraperitoneally with polyinosinic:polycytidylic acid (pIC; Sigma-Aldrich, St Louis, MO, USA) (2 μg/g body weight) on three consecutive days (days −3, −2 and −1); pIC was dissolved in Dulbecco's PBS. Rats received a single i.p. dose of 1×10^7 plaque-forming units of Kilham rat virus (KRV) on day 0. Control rats received i.p. injections of PBS on the same days. Beginning at day 10 or 11 after KRV treatment, rats were tested for glycosuria (Clinistix; Bayer, Elkhart, IN, USA). Diabetes was confirmed by blood glucose concentration >14 mmol/l on two consecutive days (Accu-Chek Aviva; Roche Diagnostics, Indianapolis, IN, USA).

Islet isolation In some experiments, pancreatic islets from BBDR rats were harvested by collagenase digestion as previously described [14]. Freshly isolated islets were snap frozen with liquid nitrogen and stored at −80°C until use.

Immunoblot analysis Rat islets were lysed with T-PER tissue protein extraction reagent (Thermo Scientific, Rockford, IL, USA) and protein concentrations were determined by bicinchoninic acid protein assay (Sigma-Aldrich). Protein samples were mixed with 4× SDS-PAGE loading buffer (240 mmol/l Tris/HCl pH 6.8, 40% glycerol, 8% SDS, 0.04% bromophenol blue, and 5% beta-mercaptoethanol) and loaded onto 4–20% pre-cast Tris-glycine gradient gels (Invitrogen, Grand Island, NY, USA) along with ladder marker (Gibco, Grand Island, NY, USA) and run at 150 V for 1.5 h. Gels were transferred onto nitrocellulose membranes with iBlot (Invitrogen), blocked with 5% non-fat milk for 1 h and placed in primary antibody overnight at 4°C. Membranes were washed three times in Tris-buffered saline Tween (TBST) and placed in secondary antibody at room temperature for 1 h. Membranes were washed three times in TBST, developed with enhanced chemiluminescence (Gibco) and imaged using Kodak chemiluminescent film. Densitometric analyses were performed with Photoshop, all protein levels were normalised to actin levels and presented as average ± SD.

Immunofluorescence staining Rat pancreas specimens were frozen in Tissue-Tek O.C.T. (Sakura Finetek USA, Torrance, CA, USA) with liquid nitrogen. Sections 5 μm thick were cut with a cryostat (Leica, Buffalo Grove, IL, USA) and stored at −80°C. Sections were fixed before staining with a mixture of ethanol and 0.1% of trichloroacetic acid for 15 min, then blocked with PBS-AT (500 ml PBS, 10 g BSA grade J and 12.5 ml of 20% Triton X-100). Sections were incubated with primary and secondary antibodies at room temperature for 1 h, separated by three washes in PBS. Mounting medium (Vectashield with DAPI; Vector Laboratories, Burlingame, CA, USA) was added to the sections after three washes in PBS. Images were captured using spinning disk confocal microscopy on a Nikon Eclipse TE2000-E microscope (Melville, NY, USA) and analysed using MetaMorph software (Molecular Devices, Downington, PA, USA).

Antibodies The following antibodies were used for immunoblots: rabbit anti-human phosphospecific (Ser724) IRE-1α (Novus, Littleton, CO, USA); rabbit anti-human IRE-1α, rabbit anti-mouse caspase-12 and rabbit anti-mouse phospho-PERK (p-PERK, Thr980, 16F8) (Cell Signaling, Danvers, MA, USA); rabbit anti-human XBP-1, rabbit anti-PKR, rabbit anti-p-eIF2a (Ser51) and rabbit anti-human PERK (Abcam, Cambridge, MA, USA); mouse anti-human ATF6 (Imgenex, San Diego, CA, USA) and rabbit anti-human caspase-3 (H-277), rabbit anti-mouse CHOP (F-168) and rabbit anti-insulin (Santa Cruz Biotechnology, Dallas, TX, USA). Mouse anti-actin (Chemicon International, Billerica, MA, USA) was used as a loading control. Secondary antibodies, anti-rabbit and anti-mouse IgG–horseradish peroxidase conjugates were from Santa Cruz Biotechnology.

For immunofluorescence staining, in addition to the antibodies described above, frozen sections were stained with mouse anti-insulin (Sigma-Aldrich), guinea pig anti-insulin (Dako, Carpinteria, CA, USA) and chicken anti-insulin (Abcam). Secondary antibodies, Alexa Fluor 488 and 592 goat anti-mouse, anti-rabbit, anti-guinea pig and anti-chicken were from Invitrogen. Isotype controls were from Pharmingen (San Diego, CA, USA).

Statistical analysis Statistical analysis was performed by Kaplan–Meier or unpaired *t* test using GraphPad Prism 5 (GraphPad Software, La Jolla, CA, USA). A *p* value of less than 0.05 was considered to be statistically significant.

Results

Insulitis and diabetes onset in virus-induced BBDR rats follow a predictable time course We had reported previously that the kinetics of type 1 diabetes development in the virus-inducible BBDR rat model follows a consistent time course [12, 13]. To confirm this finding we treated BBDR rats with KRV + pIC or PBS; as expected, most KRV + pIC-treated rats progressed to diabetes by day 14 (Fig. 1). In addition, we assessed pancreatic islet morphology at selected time points following treatment (see ESM Methods). Haematoxylin and eosin (H&E) staining of pancreas sections demonstrated that insulitis was first detectable at day 11 following KRV + pIC treatment, with more severe insulitis by day 14 (ESM Fig. 1a). Consistent with our H&E staining, islet-infiltrating CD3-positive T lymphocytes were first observed at day 11, with considerable infiltration by day 14 (ESM Fig. 1b). Based on these data and our earlier studies, we chose to investigate ER stress signalling pathways in pancreatic beta cells at discrete time points: day 4 and day 7 post infection but before development of insulitis and days 11–14 during the onset and progression of insulitis but before the development of overt hyperglycaemia.

IRE1 phosphorylation and downstream activation of X-box-binding protein 1 start at early, pre-insulitic stages and continue throughout diabetes development To investigate the occurrence of beta cell ER stress signalling during the development of virus-induced type 1 diabetes, we first examined the IRE1 pathway. Immunoblot analysis showed that active (phosphorylated) IRE1 was undetectable in lysates of pancreatic islets isolated from PBS-treated control rats, whereas IRE1 was highly active (phosphorylated) in islets isolated from rats at day 4 following KRV + pIC treatment, indicating upregulated IRE1 signalling (Fig. 2a). The ratio of phosphorylated to total IRE-1 in islets from KRV + pIC-treated rats was maintained through to day 7, as well as during later insulitic stages (day 11–14) of diabetes development (Fig. 2b).

An important downstream component in the IRE1 pathway is X-box-binding protein 1 (XBP-1). Activated IRE1 has an endoribonuclease activity, which generates a spliced, active form of XBP-1 that can translocate to the nucleus [15]. Expression of the active (spliced) form of XBP-1 was upregulated at day 4 post infection and was sustained throughout diabetes induction, whereas the level in control rats was undetectable (Fig. 3a, b). Levels of the inactive (unspliced) form of XBP-1

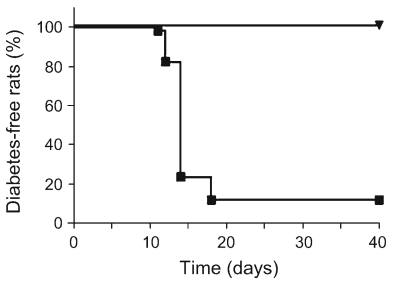

Fig. 1 BBDR rats treated with KRV + pIC develop autoimmune type 1 diabetes with a predictable time course. BBDR rats were monitored for development of diabetes following KRV + pIC treatment; shown is a Kaplan–Meier plot for KRV + pIC- ($n = 51$, squares) compared with PBS-treated rats ($n = 12$, triangles), ***$p < 0.001$

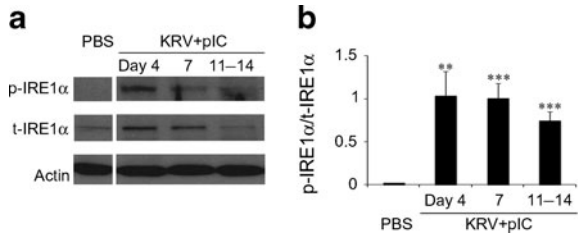

Fig. 2 IRE-1α phosphorylation occurs at an early stage of diabetes induction. (**a**) Immunoblot of protein lysates of isolated pancreatic islets from PBS (control)- or KRV + pIC-treated rats for the phosphorylated form of IRE-1α (p-IRE-1α, Ser724) and total IRE-1α (t-IRE-1α); actin was used as loading control. (**b**) Densitometric analysis (average ± SD, $n=3$) of p-IRE-1α/t-IRE-1α ratio; $^{**}p<0.01$ and $^{***}p<0.001$ compared with PBS-treated rats

were similar in both control and diabetes-induced rats. To verify XBP-1 activation specifically in pancreatic beta cells, we stained pancreas sections from control and KRV + pIC-treated rats for insulin and XBP-1. Pancreas sections from KRV + pIC-treated rats showed distinct nuclear XBP-1 staining in insulin-positive beta cells throughout diabetes induction, consistent with XBP-1 activation, while the staining in PBS-treated rats was negligible (Fig. 3c). Interestingly, alpha cells have recently been reported to undergo ER stress [16]; we also observed activated (nuclear) XBP-1 staining in glucagon-positive alpha cells of KRV + pIC-treated rats (ESM Fig. 2).

ER stress-specific caspase 12 activation occurs at early, pre-insulitic stages in pancreatic islets of KRV + pIC-treated rats Caspase 12 is an ER-localised pro-apoptotic protein that is activated specifically through the IRE1 signalling pathway in response to pathological ER stress [17, 18]. We investigated whether upregulated IRE1 signalling in the islets of virus-induced BBDR rats had transitioned to pathological ER stress by measuring the expression of the activated (cleaved) form of pro-apoptotic caspase 12. Elevated levels of activated caspase 12 were found in isolated islets of KRV + pIC-treated rats beginning at day 4, well before the onset of insulitis, as well as at day 7 and later, insulitic stages (day 11–14) of diabetes induction (Fig. 4a, b).

To determine caspase 12 expression specifically in beta cells, we co-stained pancreatic sections from PBS (control)- and KRV + pIC-treated rats for insulin and caspase 12. Islets from control rats showed robust insulin expression with very low or undetectable staining for caspase 12 (Fig. 4c). In contrast, by day 14 of virus infection, we observed that many islets consisted of beta cells with dramatically increased

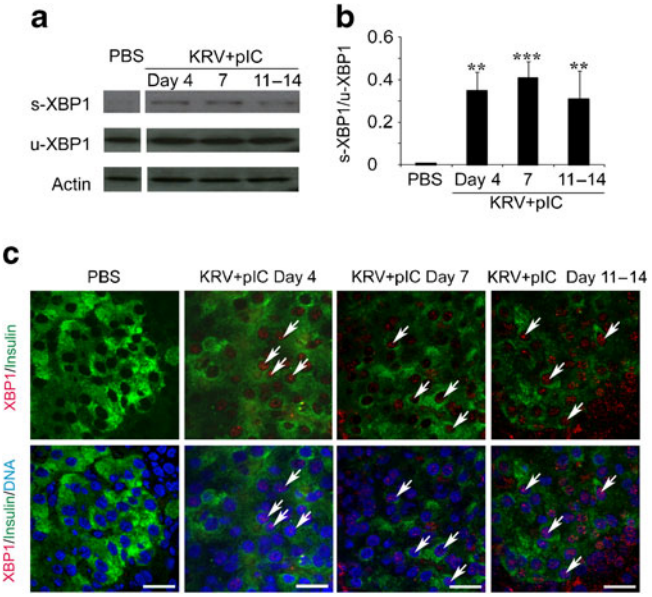

Fig. 3 Activation of XBP-1 occurs at an early stage of diabetes induction. (**a**) Immunoblot of protein lysates of isolated pancreatic islets from PBS (control)- or KRV + pIC-treated rats for the spliced (s) and unspliced (u) forms of XBP-1 (XBP1); actin was used as loading control. (**b**) Densitometric analysis (average ± SD, $n=3$) of s-XBP1/u-XBP1 ratio; $^{**}p<0.01$ and $^{***}p<0.001$ compared with PBS-treated rats. (**c**) Immunofluorescence staining of frozen pancreas tissues; upper panels show staining with XBP-1 (XBP1, red) and insulin (green), lower panels show overlay with DAPI (blue) to visualise the nuclei. Arrows indicate beta cells positive for XBP-1 nuclear translocation. Representative immunofluorescence staining is shown; $n=4$ rats at each time point; at least three fields were examined for each rat. Magnification, ×40; scale bar, 20 μm

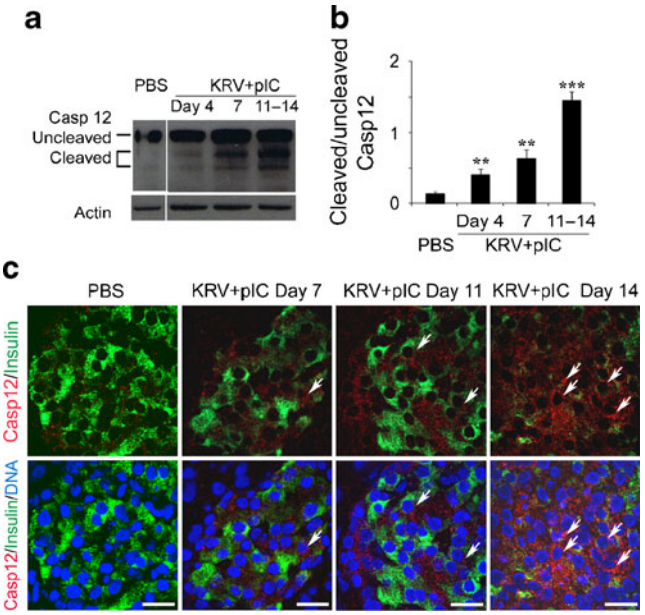

Fig. 4 Activation of ER stress-specific caspase 12 in pancreatic islets of diabetes-induced BBDR rats occurs before the onset of insulitis. (**a**) Caspase 12 (Casp 12) immunoblot of protein lysates of isolated pancreatic islets from PBS (control)- or KRV + pIC-treated rats; actin was used as loading control. (**b**) Densitometric analysis (average ± SD, $n=3$) of cleaved/uncleaved caspase 12 ratio; $^{**}p<0.01$ and $^{***}p<0.001$ compared with PBS-treated rats. (**c**) Immunofluorescence staining of frozen pancreas tissues; upper panels show staining for caspase 12 (red) and insulin (green), lower panels show overlay with DAPI (blue) to visualise the nuclei. Arrows indicate beta cells with positive caspase 12 staining. Representative immunofluorescence staining is shown; $n=4$ rats at each time point; at least three fields were examined for each rat. Magnification, ×40; scale bar, 20 μm

caspase 12 staining in conjunction with greatly reduced insulin levels.

Activation of effector caspase 3 occurs before insulitis in pancreatic islets of KRV + pIC-treated rats We also examined the activation of caspase 3, the main effector caspase of apoptotic cell death, in pancreatic islets isolated from PBS (control)- and KRV + pIC-treated rats. We observed a marked increase in the active (cleaved) form of caspase 3 at day 7 of KRV + pIC treatment, demonstrating that pancreatic islets undergo apoptosis before the development of insulitis in this virus-inducible diabetes model (Fig. 5). Caspase 3 activation was also high at late stages. In contrast, only the inactive (uncleaved) form of caspase 3 was observed in islets from PBS-treated rats. To confirm apoptosis by a different method, we stained pancreas sections from control and treated rats for TUNEL. We found an increase in the numbers of TUNEL-positive beta cells in the pancreas sections from KRV + pIC-treated rats both before and during insulitis (ESM Fig. 3). Together with our caspase 12 results described above, these data demonstrate that pro-apoptotic ER stress and pancreatic beta cell death first occur before the insulitic event, suggesting a role for pathological ER stress in the very early stages of virus-induced diabetes.

PERK phosphorylation and the pro-apoptotic ER stress marker, CHOP, are highly increased in pancreatic islets only at the late, insulitic stage of diabetes induction We next examined the PERK pathway and found that PERK was present in islet lysates from both control and treated rats at similar levels. The active (phosphorylated) form of PERK was moderately increased at day 7, but the highest levels of activation were seen at days 11–14 when lymphocytic infiltration was occurring (Fig. 6). In addition we analysed the islet protein lysates for ATF4, a downstream transcription factor in the PERK pathway [19], but we observed little difference in ATF4 expression in islets from control or KRV + pIC-treated rats (Fig. 7).

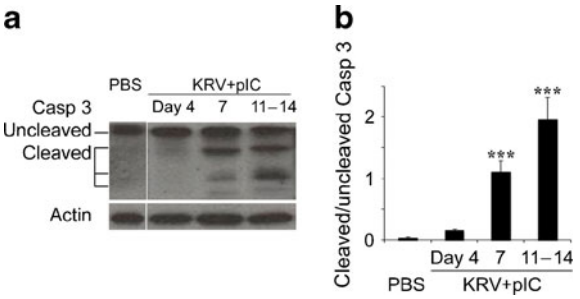

Fig. 5 Activation of caspase 3 in pancreatic islets of diabetes-induced BBDR rats occurs before the onset of insulitis. (**a**) Caspase 3 (Casp 3) immunoblot of protein lysates of isolated pancreatic islets from PBS (control)- or KRV + pIC-treated rats; actin was used as loading control. (**b**) Densitometric analysis (average ± SD, $n=3$) of cleaved/uncleaved caspase 3 ratio; ***$p<0.001$ compared with PBS-treated rats

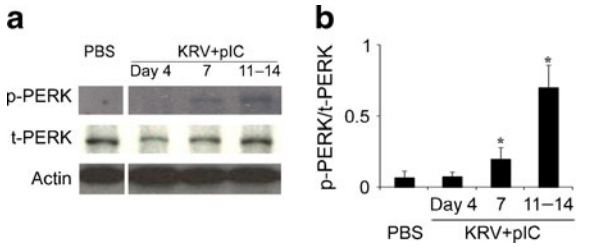

Fig. 6 PERK pathway activation in pancreatic islets occurs mainly at late stages of diabetes induction. (**a**) Immunoblot of protein lysates of isolated pancreatic islets from PBS (control)- or KRV + pIC-treated rats for the phosphorylated active form of PERK (p-PERK, Thr980) and total PERK (t-PERK); actin was used as loading control. (**b**) Densitometric analysis (average ± SD, $n=3$) of p-PERK/t-PERK ratio; *$p<0.05$ compared with PBS-treated rats

Activated PERK inhibits cellular mRNA translation by directly phosphorylating the eukaryotic translation initiation factor, eIF2α [4]; eIF2α can also be phosphorylated by PKR, which is activated by double-stranded RNA such as synthetic pIC [20, 21]. We found that PKR expression in islets of KRV + pIC-treated rats trended higher at day 7, $p=0.06$ (Fig. 8). We next analysed our islet protein lysates for eIF2α phosphorylation. However, immunoblot analysis of control and KRV + pIC-treated rat islets showed that they exhibited relatively

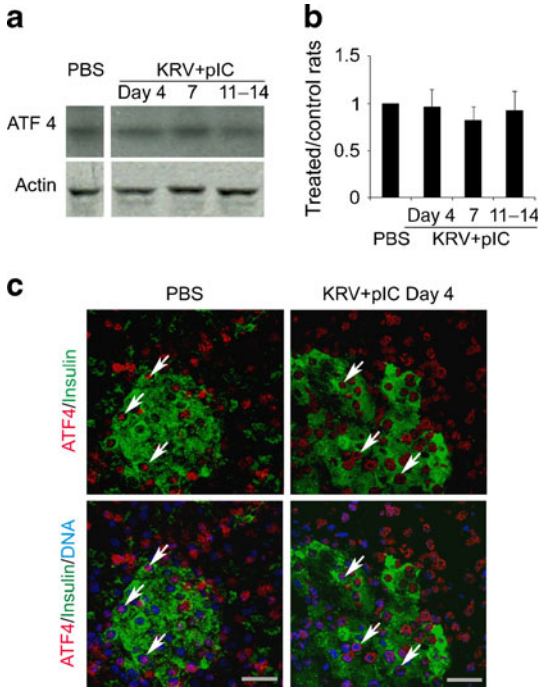

Fig. 7 Expression of ATF4 is not significantly affected during induction of diabetes. (**a**) ATF4 immunoblot of protein lysates of isolated pancreatic islets from PBS (control)- or KRV + pIC-treated rats; actin was used as loading control. (**b**) Densitometric analysis (average ± SD, $n=3$) of ATF4. (**c**) Immunofluorescence staining of frozen pancreas tissues; upper panels show staining with ATF4 (red) and insulin (green), lower panels show overlay with DAPI (blue) to visualise the nuclei. Representative immunofluorescence staining is shown; $n=4$ rats at each time point, at least three fields were examined for each rat. Magnification, ×40; scale bar, 30 μm

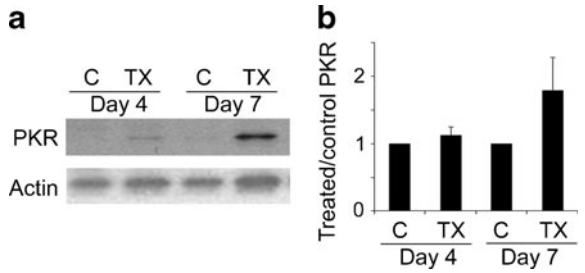

Fig. 8 Expression of PKR is increased in KRV + pIC-treated rats. (**a**) PKR immunoblot of protein lysates of isolated pancreatic islets from PBS-treated control (C) or KRV + pIC-treated (TX) rats; actin was used as loading control. (**b**) Densitometric analysis (average ± SD, $n=3$) of treated/control ratio of PKR (normalised to actin)

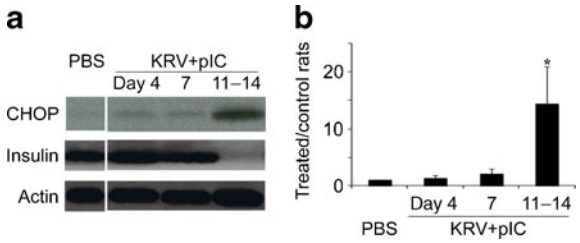

Fig. 10 Pro-apoptotic CHOP expression in pancreatic islets occurs mainly at late stages of diabetes induction. Pancreatic tissues from BBDR rats treated with KRV + pIC or PBS (control) were recovered at the time points indicated. (**a**) Immunoblot of protein lysates of isolated pancreatic islets from PBS- or KRV + pIC-treated rats; actin was used as loading control. (**b**) Densitometric analysis (average ± SD, $n=3$) of CHOP; *$p<0.05$ compared with PBS-treated rats

similar levels of eIF2α phosphorylation (Fig. 9). Together with our ATF4 results, these data suggest that pancreatic islets normally exhibit high physiological UPR activity.

We measured the expression of CHOP (CCAAT/-enhancer-binding-protein homologous protein), which is regulated by the PERK pathway and acts to induce apoptosis during prolonged ER stress [3, 19, 22, 23]. Immunoblot analysis of isolated islets revealed that CHOP expression was highly elevated only at the late stage during autoreactive T lymphocyte infiltration (Fig. 10a, b). Concomitant with high levels of CHOP expression, we found marked reductions in the level of intracellular insulin (Fig. 10a), consistent with significant beta cell dysfunction or death at this stage.

Expression and activation of ATF6 is not significantly affected by diabetes induction Finally, we examined the third major ER stress transducer, ATF6. Upon ER stress, ATF6 translocates from the ER to the Golgi where it is cleaved and then travels to the nucleus to activate transcription of downstream ER stress target genes [24, 25]. Immunoblot analysis of pancreatic islets isolated from control and KRV + pIC-treated rats showed high levels of ATF6 in both groups (Fig. 11a, b); nuclear translocation of ATF6 in beta cells was also similar in control and treated rats (Fig. 11c). These data demonstrate that although pancreatic beta cells express robust levels of ATF6 (presumably a reflection of their high insulin load), the expression levels and activation (nuclear translocation) of ATF6 were not significantly altered with diabetes induction.

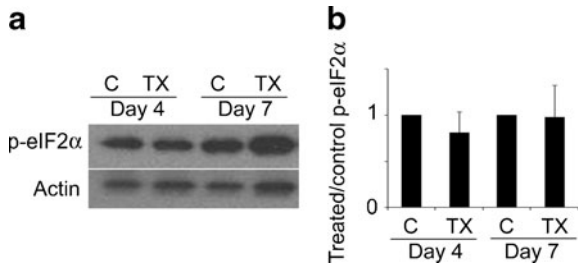

Fig. 9 Expression of phosphorylated eIF2α is similar in control and KRV + pIC-treated rats. (**a**) Phosphorylated eIF2α (p-eIF2α) immunoblot of protein lysates of isolated pancreatic islets from PBS-treated control (C) or KRV + pIC-treated (TX) rats; actin was used as loading control. (**b**) Densitometric analysis (average ± SD, $n=3$) of treated/control ratio of p-eIF2α (normalised to actin)

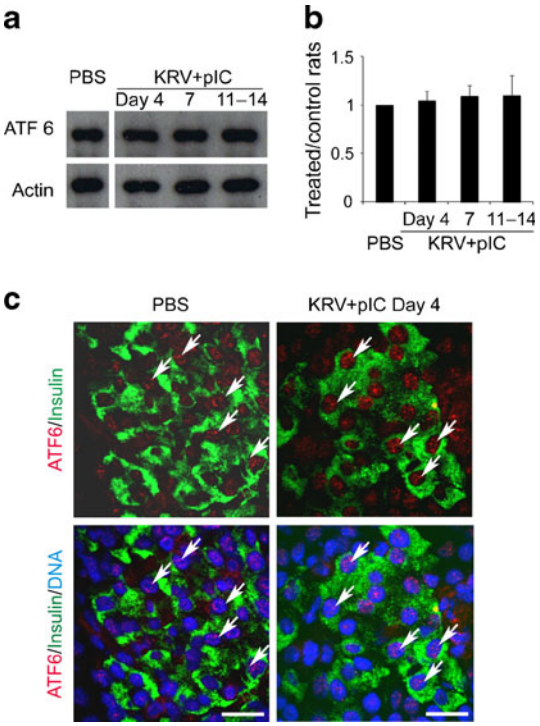

Fig. 11 High basal expression of ATF6 is not affected by diabetes induction. (**a**) ATF6 immunoblot of protein lysates of isolated pancreatic islets from PBS-treated (control) or KRV + pIC-treated rats; actin was used as loading control. (**b**) Densitometric analysis (average ± SD, $n=3$) of ATF6. (**c**) Immunofluorescence staining of frozen pancreas tissues; upper panels show staining for ATF6 (red) and insulin (green), lower panels show overlay with DAPI (blue) to visualise the nuclei. Arrows indicate beta cells with positive ATF6 nuclear translocation. Representative immunofluorescence staining is shown; $n=4$ rats at each time point, at least three fields were examined for each rat. Magnification, ×40; scale bar, 20 μm

Discussion

In this study we used the KRV + pIC-inducible BBDR rat model to investigate a role for pancreatic beta cell ER stress during the development of virus-induced type 1 diabetes. We systematically analysed the three major ER stress pathways and focused on early stages in diabetes development (days 4 and 7), before the development of histologically and immunologically detectable insulitis, and on a late stage (days 11–14) corresponding to the onset and progression of insulitis, but before the development of diabetes. Here we report specific activation of the IRE1 pathway and its downstream component XBP-1 at early, pre-insulitic stages of diabetes development. Importantly, we found that pro-apoptotic caspase 12, a downstream effector of pathological IRE1 signalling, was also activated during this stage. These data demonstrate that pathological ER stress contributes to early-stage beta cell death well before the infiltration of autoreactive lymphocytes in this virus-induced model of type 1 diabetes.

Of note, viral infections have long been implicated as important factors in the aetiology and/or pathogenesis of type 1 diabetes in HLA-susceptible individuals [26–28]; further, polymorphisms in the *IFIH1* gene have been convincingly associated with type 1 diabetes [11, 29]. *IFIH1* encodes for the interferon-induced helicase C domain-containing protein-1 that detects double-stranded RNA produced by certain viruses and mediates an antiviral response [30]. In the genetically susceptible BBDR rat the mechanism underlying the development of autoimmune diabetes following exposure to KRV infection remains incompletely understood. KRV infects lymphoid tissue but does not directly infect pancreatic islets [31, 32]; co-treatment with pIC, a synthetic double-stranded RNA, greatly increases the incidence of diabetes [12, 33]. In the BBDR rat, KRV + pIC treatment causes a potent innate immune response mediated by Toll-like receptor proteins TLR9 and TLR3, respectively, and results in a rapid upregulation of multiple pro-inflammatory cytokines and chemokines [34–36].

In our study, specific in vivo activation of IRE1 and its downstream effector XBP-1 occurred at early stages of diabetes induction when beta cells were exposed to these multiple pro-inflammatory cytokines and chemokines. This is consistent with earlier reports that in vitro exposure of beta cells to cytokines leads to the induction of ER stress [37, 38]. We also found increased levels of haem oxygenase-1 (HO-1), indicative of oxidative stress, in islet lysates from rats at days 4 and 7 of KRV + pIC treatment (data not shown). Prolonged exposure of the pancreatic islets of KRV + pIC-treated rats to these cytotoxic insults may underlie the transition to pathological ER stress and beta cell apoptosis [17], as we also observed activation of pro-apoptotic caspase 12 specifically in beta cells during this early stage of diabetes induction. Indeed, although the human orthologue of caspase 12 is non-functional due to deleterious mutations in its open reading frame [39], in rodents caspase 12 belongs to the subgroup of inflammatory caspases [40, 41]. Importantly, caspase 12 is the sole caspase localised to the ER and it is activated specifically through the IRE1 signalling pathway [17, 18].

Caspase 12, in turn, is involved in the apoptotic cascade that activates the downstream effector caspase 3 [42, 43]. In our study, caspase 3 was activated at early stages of diabetes induction and, although we cannot rule out that other apoptotic pathways may also be involved in caspase 3 activation, our data suggest that pathological IRE1 signalling likely plays a contributory role in this early beta cell death. In support of this, we (and others) have recently reported that thioredoxin-interacting protein (TXNIP) is a possible link between pathological ER stress, especially via the IRE1 pathway, and inflammasome activation and IL-1β production, which in turn promote beta cell apoptosis [44, 45]. Indeed, consistent with these reports, IL-1β expression was detected in isolated islets of BBDR rats before the development of insulitis (day 7 of KRV + pIC treatment, data not shown). In an earlier report, we also found that exposure of beta cells to chronic hyperglycaemia in vitro caused IRE1 activation and an accompanying decrease in insulin production [46]. However, the initial activation of IRE1 in our current study was not a consequence of hyperglycaemia, as treated rats maintained normal blood glucose levels during this early stage of diabetes progression.

During the late insulitic stage of diabetes induction, activated caspase 12 remained elevated along with a dramatic induction of the pro-apoptotic protein CHOP. CHOP deletion has been shown to promote beta cell survival in several mouse models of diabetes, consistent with its pro-apoptotic function [23, 47, 48]. CHOP induction in our rat model primarily occurred only at late stages of diabetes induction, when lymphocytic infiltration was robust. Consistent with this, Tersey et al [11] recently reported that ER stress-responsive genes, including CHOP and active (spliced) XBP-1, were upregulated in the pancreatic islets of NOD mice during the insulitic stage, but before diabetes onset; this correlated with the decreased insulin production and relative glucose intolerance of the NOD compared with diabetes-resistant mouse strains. Interestingly, expression levels of CHOP were also increased in islets from individuals with type 1 diabetes compared with non-diabetic controls, although there was no difference observed in XBP-1 levels [10]. Together, these data demonstrate that multiple ER stress pathways contribute to pancreatic islet destruction during infiltration of autoreactive lymphocytes.

In summary, we used the virus-inducible BBDR rat model to investigate in vivo ER stress signalling in pancreatic beta cells during development of autoimmune type 1 diabetes. Following diabetes induction, the IRE1 pathway and caspase 12 were specifically activated at early time points well before the development of insulitis. Our data support a scenario in which pathological IRE1-mediated ER stress signalling and activation of pro-apoptotic molecules contribute to early

pancreatic beta cell damage, which may, in turn, release beta cell autoantigens that elicit or exacerbate the autoreactive immune attack and ultimately mediate the complete destruction of the beta cells [49]. This report highlights the IRE1 ER stress pathway as a unique target in the early initiation and progression of virus-induced type 1 diabetes.

Acknowledgements We thank Aldo A. Rossini from Joslin Diabetes Center, Boston, USA, for helpful discussions and insights. We also thank Elaine Norowski and Linda Leehy (Program in Molecular Medicine) for their outstanding technical assistance and Paul Furcinitti (Digital Light Microscopy Core Facility) at the University of Massachusetts Medical School, Worcester, USA, for assistance with spinning disk confocal microscopy.

Funding This work was supported by National Institutes of Health Grants AI046629, the Beta Cell Biology Consortium DK72473 and grants from the JDRF International, the Helmsley Foundation and the Brehm Foundation. Core resources supported by the NIH Diabetes Endocrinology Research Center grant (DK32520) were used.

The contents of this publication are solely the responsibility of the authors and do not necessarily represent the official views of the National Institutes of Health.

Duality of interest The authors declare that there is no duality of interest associated with this manuscript.

Contribution statement CY designed and performed research, analysed the data and wrote the manuscript. PD and AJ performed research and revised and reviewed the manuscript, BO-M and FU contributed to the study design and revised and reviewed the manuscript and RB designed the study, analysed the data and wrote the manuscript. All authors approved the final version of the manuscript.

References

1. Wu J, Kaufman RJ (2006) From acute ER stress to physiological roles of the Unfolded Protein Response. Cell Death Differ 13:374–384
2. Bertolotti A, Zhang Y, Hendershot LM, Harding HP, Ron D (2000) Dynamic interaction of BiP and ER stress transducers in the unfolded-protein response. Nat Cell Biol 2:326–332
3. Schroder M, Kaufman RJ (2005) ER stress and the unfolded protein response. Mutat Res 569:29–63
4. Ron D, Walter P (2007) Signal integration in the endoplasmic reticulum unfolded protein response. Nat Rev Mol Cell Biol 8:519–529
5. Luo D, He Y, Zhang H et al (2008) AIP1 is critical in transducing IRE1-mediated endoplasmic reticulum stress response. J Biol Chem 283:11905–11912
6. Araki E, Oyadomari S, Mori M (2003) Impact of endoplasmic reticulum stress pathway on pancreatic beta-cells and diabetes mellitus. Exp Biol Med (Maywood) 228:1213–1217
7. Oslowski CM, Urano F (2010) The binary switch between life and death of endoplasmic reticulum-stressed beta cells. Curr Opin Endocrinol Diabetes Obes 17:107–112
8. Eizirik DL, Cardozo AK, Cnop M (2008) The role for endoplasmic reticulum stress in diabetes mellitus. Endocr Rev 29:42–61
9. Marchetti P, Bugliani M, Lupi R et al (2007) The endoplasmic reticulum in pancreatic beta cells of type 2 diabetes patients. Diabetologia 50:2486–2494
10. Marhfour I, Lopez XM, Lefkaditis D et al (2012) Expression of endoplasmic reticulum stress markers in the islets of patients with type 1 diabetes. Diabetologia 55:2417–2420
11. Tersey SA, Nishiki Y, Templin AT et al (2012) Islet beta-cell endoplasmic reticulum stress precedes the onset of type 1 diabetes in the nonobese diabetic mouse model. Diabetes 61:818–827
12. Mordes JP, Bortell R, Blankenhorn EP, Rossini AA, Greiner DL (2004) Rat models of type 1 diabetes: genetics, environment, and autoimmunity. ILAR J 45:278–291
13. Kruger AJ, Yang C, Lipson KL et al (2011) Leptin treatment confers clinical benefit at multiple stages of virally induced type 1 diabetes in BB rats. Autoimmunity 44:137–148
14. Gottlieb PA, Berrios JP, Mariani G et al (1990) Autoimmune destruction of islets transplanted into RT6-depleted diabetes-resistant BB/Wor rats. Diabetes 39:643–645
15. Yoshida H, Oku M, Suzuki M, Mori K (2006) pXBP1(U) encoded in XBP1 pre-mRNA negatively regulates unfolded protein response activator pXBP1(S) in mammalian ER stress response. J Cell Biol 172:565–575
16. Akiyama M, Liew CW, Lu S et al (2013) X-box binding protein 1 is essential for insulin regulation of pancreatic alpha-cell function. Diabetes 62:2439–2449
17. Szegezdi E, Fitzgerald U, Samali A (2003) Caspase-12 and ER-stress-mediated apoptosis: the story so far. Ann N Y Acad Sci 1010:186–194
18. Nakagawa T, Zhu H, Morishima N et al (2000) Caspase-12 mediates endoplasmic-reticulum-specific apoptosis and cytotoxicity by amyloid-beta. Nature 403:98–103
19. Harding HP, Novoa I, Zhang Y et al (2000) Regulated translation initiation controls stress-induced gene expression in mammalian cells. Mol Cell 6:1099–1108
20. Hotamisligil GS (2010) Endoplasmic reticulum stress and the inflammatory basis of metabolic disease. Cell 140:900–917
21. Nakamura T, Furuhashi M, Li P et al (2010) Double-stranded RNA-dependent protein kinase links pathogen sensing with stress and metabolic homeostasis. Cell 140:338–348
22. Wang XZ, Lawson B, Brewer JW et al (1996) Signals from the stressed endoplasmic reticulum induce C/EBP-homologous protein (CHOP/GADD153). Mol Cell Biol 16:4273–4280
23. Oyadomari S, Takeda K, Takiguchi M et al (2001) Nitric oxide-induced apoptosis in pancreatic beta cells is mediated by the endoplasmic reticulum stress pathway. Proc Natl Acad Sci U S A 98:10845–10850
24. Haze K, Yoshida H, Yanagi H, Yura T, Mori K (1999) Mammalian transcription factor ATF6 is synthesized as a transmembrane protein and activated by proteolysis in response to endoplasmic reticulum stress. Mol Biol Cell 10:3787–3799
25. Thomas SE, Dalton LE, Daly ML, Malzer E, Marciniak SJ (2010) Diabetes as a disease of endoplasmic reticulum stress. Diabetes Metab Res Rev 26:611–621
26. Akerblom HK, Vaarala O, Hyoty H, Ilonen J, Knip M (2002) Environmental factors in the etiology of type 1 diabetes. Am J Med Genet 115:18–29
27. Nairn C, Galbraith DN, Taylor KW, Clements GB (1999) Enterovirus variants in the serum of children at the onset of type 1 diabetes mellitus. Diabet Med 16:509–513
28. von Herrath MG, Holz A, Homann D, Oldstone MB (1998) Role of viruses in type I diabetes. Semin Immunol 10:87–100
29. Nejentsev S, Walker N, Riches D, Egholm M, Todd JA (2009) Rare variants of IFIH1, a gene implicated in antiviral responses, protect against type 1 diabetes. Science 324:387–389
30. Chistiakov DA (2010) Interferon induced with helicase C domain 1 (IFIH1) and virus-induced autoimmunity: a review. Viral Immunol 23:3–15
31. Brown DW, Welsh RM, Like AA (1993) Infection of peripancreatic lymph nodes but not islets precedes Kilham rat virus-induced diabetes in BB/Wor rats. J Virol 67:5873–5878

32. Zipris D (2009) Epidemiology of type 1 diabetes and what animal models teach us about the role of viruses in disease mechanisms. Clin Immunol 131:11–23
33. Mordes JP, Bortell R, Doukas J et al (1996) The BB/Wor rat and the balance hypothesis of autoimmunity. Diabetes Metab Rev 12:103–109
34. Zipris D, Lien E, Nair A et al (2007) TLR9-signaling pathways are involved in Kilham rat virus-induced autoimmune diabetes in the biobreeding diabetes-resistant rat. J Immunol 178:693–701
35. Zipris D, Lien E, Xie JX, Greiner DL, Mordes JP, Rossini AA (2005) TLR activation synergizes with Kilham rat virus infection to induce diabetes in BBDR rats. J Immunol 174:131–142
36. Zipris D (2011) Innate immunity in type 1 diabetes. Diabetes Metab Res Rev 27:824–829
37. Chambers KT, Unverferth JA, Weber SM, Wek RC, Urano F, Corbett JA (2008) The role of nitric oxide and the unfolded protein response in cytokine-induced beta-cell death. Diabetes 57:124–132
38. Cardozo AK, Ortis F, Storling J et al (2005) Cytokines downregulate the sarcoendoplasmic reticulum pump Ca2+ ATPase 2b and deplete endoplasmic reticulum Ca2+, leading to induction of endoplasmic reticulum stress in pancreatic beta-cells. Diabetes 54:452–461
39. Fischer H, Koenig U, Eckhart L, Tschachler E (2002) Human caspase 12 has acquired deleterious mutations. Biochem Biophys Res Commun 293:722–726
40. Nadiri A, Wolinski MK, Saleh M (2006) The inflammatory caspases: key players in the host response to pathogenic invasion and sepsis. J Immunol 177:4239–4245
41. Scott AM, Saleh M (2007) The inflammatory caspases: guardians against infections and sepsis. Cell Death Differ 14:23–31
42. Hitomi J, Katayama T, Taniguchi M, Honda A, Imaizumi K, Tohyama M (2004) Apoptosis induced by endoplasmic reticulum stress depends on activation of caspase-3 via caspase-12. Neurosci Lett 357:127–130
43. Kerbiriou M, Teng L, Benz N, Trouve P, Ferec C (2009) The calpain, caspase 12, caspase 3 cascade leading to apoptosis is altered in F508del-CFTR expressing cells. PLoS One 4:e8436
44. Oslowski CM, Hara T, O'Sullivan-Murphy B et al (2012) Thioredoxin-interacting protein mediates ER stress-induced beta cell death through initiation of the inflammasome. Cell Metab 16: 265–273
45. Lerner AG, Upton JP, Praveen PV et al (2012) IRE1alpha induces thioredoxin-interacting protein to activate the NLRP3 inflammasome and promote programmed cell death under irremediable ER stress. Cell Metab 16:250–264
46. Lipson KL, Fonseca SG, Ishigaki S et al (2006) Regulation of insulin biosynthesis in pancreatic beta cells by an endoplasmic reticulum-resident protein kinase IRE1. Cell Metab 4:245–254
47. Song B, Scheuner D, Ron D, Pennathur S, Kaufman RJ (2008) Chop deletion reduces oxidative stress, improves beta cell function, and promotes cell survival in multiple mouse models of diabetes. J Clin Invest 118:3378–3389
48. Oyadomari S, Mori M (2004) Roles of CHOP/GADD153 in endoplasmic reticulum stress. Cell Death Differ 11:381–389
49. Horwitz MS, Ilic A, Fine C, Rodriguez E, Sarvetnick N (2002) Presented antigen from damaged pancreatic beta cells activates autoreactive T cells in virus-mediated autoimmune diabetes. J Clin Invest 109:79–87